

## RADIO CONTINUUM SOURCES ASSOCIATED WITH THE HH 92 AND HH 34 JETS

Luis F. Rodríguez<sup>1,2</sup>, Bo Reipurth<sup>3,4</sup>, and Hsin-Fang Chiang<sup>3,4</sup>

Received 2014 April 14; accepted 2014 May 23

### RESUMEN

Presentamos observaciones de alta resolución angular y alta sensibilidad en el radiocontinuo a 8.46 GHz (3.6 cm) hacia el núcleo del flujo HH 92 hechas con el Very Large Array en 2002-2003 y con el Expanded Very Large Array en 2011. Detectamos un grupo de tres fuentes compactas distribuidas en una región con 2'' de extensión y discutimos su naturaleza. Concluimos que una de las fuentes (VLA 1) es la excitadora del flujo gigante asociado con HH 92. En el caso de HH 34 presentamos nuevas observaciones a 43.3 GHz (7 mm) que revelan la presencia de una estructura asociada con la fuente excitadora y alargada perpendicularmente al chorro óptico altamente colimado en la región. Proponemos que la fuente de 7 mm es un disco circunestelar con radio de  $\sim 80$  AU y masa de  $\sim 0.21 M_{\odot}$ .

### ABSTRACT

We present high angular resolution, high sensitivity 8.46 GHz (3.6 cm) radio continuum observations made toward the core of the HH 92 outflow with the Very Large Array in 2002-2003 and with the Expanded Very Large Array in 2011. We detect a group of three compact sources distributed in a region 2'' in extension and discuss their nature. We conclude that one of the objects (VLA 1) is the exciting source of the giant outflow associated with HH 92. In the case of HH 34 we present new 43.3 GHz (7 mm) observations that reveal the presence of a structure associated with the exciting source and elongated perpendicular to the highly collimated optical jet in the region. We propose that this 7 mm source is a circumstellar disk with radius of  $\sim 80$  AU and mass of  $\sim 0.21 M_{\odot}$ .

*Key Words:* ISM: JETS AND OUTFLOWS — STARS: FORMATION — STARS: MASS LOSS — RADIO CONTINUUM: STARS

### 1. INTRODUCTION

It is well-established that the typical outcome of the collapse of a cloud is a small multiple system (e.g. Duchêne et al. 2006; Reipurth et al. 2014). In particular, at centimeter wavelengths the studies of Reipurth et al. (2002a; 2004) have shown that the cores of regions associated with outflow activity typically reveal the presence of several radio continuum sources, each one usually believed to be tracing the presence of a recently formed star. However, these compact radio sources could also trace colli-

sionally ionized regions, that is, the radio equivalent of Herbig-Haro objects, sources without an embedded star.

In the case of forming stars of low and intermediate mass, the observed radio emission directly associated with the young star has two possible origins. A first class of sources are those with resolved structure at the scale of tenths of arc seconds that are usually emitting free-free (thermal) radiation from ionized, collimated outflows (e.g., Curiel et al. 1993). A second class of sources are young stars with magnetospheric activity that produces detectable gyrosynchrotron (non-thermal) emission (e.g., Dzib et al. 2013). The determination of the characteristics of these sources can be of great help in improving our understanding of the region studied, locating precisely the position of young stars with either outflow or magnetospheric activity. In particular, the

<sup>1</sup>Centro de Radioastronomía y Astrofísica, Universidad Nacional Autónoma de México, Campus Morelia

<sup>2</sup>Astronomy Department, Faculty of Science, King Abdulaziz University, P.O. Box 80203, Jeddah 21589, Saudi Arabia

<sup>3</sup>Institute for Astronomy, University of Hawaii at Manoa, Hilo, HI, USA

<sup>4</sup>NASA Astrobiology Institute, University of Hawaii at Manoa, Hilo, HI, USA

detection of elongated free-free sources, sometimes called thermal jets (Anglada 1996; Rodríguez 1997; Rodríguez et al. 1999; Rodríguez et al. 2000), locates the exciting source and the origin and orientation of the outflow at sub-arcsec scales. At the shortest wavelengths, e.g. 7 mm, dust emission also becomes detectable, allowing additional high resolution imaging of circumstellar material (Rodríguez et al. 2008a).

### 1.1. *The HH 92 Jet and its Driving Source*

Bally, Reipurth, & Aspin (2002) reported the detection of a highly collimated, low-excitation jet, HH 92, that emerges (with a position angle of  $311^\circ$ ) from an asymmetric infrared reflection nebula spatially related with the source IRAS 05399-0121, an embedded low-mass class I protostar with a bolometric luminosity of  $10 L_\odot$ . In their study, Bally et al. (2002) propose that HH 92, together with the well-known objects HH 90/91 and HH 93 (Reipurth 1985; 1989) trace a single giant outflow lobe  $\simeq 3$  pc in length. The driving source is located in a cloud clump labeled as LBS 30 (Lada et al. 1991) with two cores, as seen in an  $850 \mu\text{m}$  SCUBA image (Figure 1) from the SCUBA Legacy Survey (Di Francesco et al. 2008). Similar structure is seen in the  $350 \mu\text{m}$  maps of Miettinen & Offner (2013).

However, despite several early efforts the exciting source of this giant outflow was initially not firmly identified (Gredel, Reipurth, & Heathcote 1992; Davis, Mundt, & Eisloffel 1994; Reipurth et al. 1993). With the advent of the Spitzer and Herschel missions, an accurate position and photometry were achieved (Megeath et al. 2012; Manoj et al. 2013). Most recently, the source has been studied in detail at sub-mm wavelengths by Miettinen & Offner (2013), who give further references to the literature.

In this paper we present sensitive, high angular resolution Very Large Array and Expanded Very Large Array observations at 8.46 GHz (3.6 cm) of the core of the region that reveal the presence of a compact group of radio sources. A distance of 415 pc to the L1630 cloud, where HH 92 is embedded, is adopted (Anthony-Twarog 1982).

### 1.2. *HH 34 and its Driving Source*

The Herbig-Haro object HH 34 was first noted by Guillermo Haro, see Herbig (1974). It is part of a major complex of shocks, including a highly collimated jet (Reipurth et al. 1986), and distant bow shocks that make the complex span across almost 3 pc (Devine et al. 1997). Proper motions and radial velocities indicate a dynamic age of the entire complex of about 10,000 yr (Devine et al. 1997, Reipurth

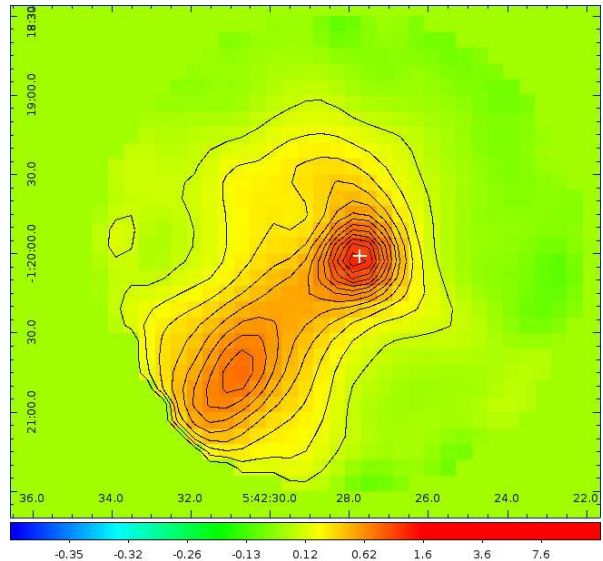


Fig. 1. An  $850 \mu\text{m}$  SCUBA map of the filamentary cloud clump LBS 30 in which the HH 92 driving source is located (white cross). The elongated cloud clump has fragmented into two separate cores, of which only the north-western has begun to form stars (Miettinen & Offner 2013). The cross has the same dimensions ( $4.5'' \times 4.5''$ ) as the panels in Figure 2.

et al. 2002b). The driving source is not optically visible, although a compact reflection nebula is visible at the base of the jet, and spectroscopy of this nebula shows that the source is a rich emission-line T Tauri star (Reipurth et al. 1986). Imaging with NICMOS on HST reveals the driving source in the H- and K-bands (Reipurth et al. 2000). The source was also detected with low spatial resolution in the radio continuum at 3.6 cm (Rodríguez & Reipurth 1996). HH 34 is located in the northern part of the L1641 cloud, just south of the Orion Nebula cluster, whose distance has been determined as  $414 \pm 7$  pc by Menten et al. (2007) and  $418 \pm 6$  pc by Kim et al. (2008), see also the discussion in Muench et al. (2008). We here use the mean distance of 416 pc.

In this paper we present a deep high angular resolution radio continuum VLA map obtained at 7 mm.

## 2. OBSERVATIONS

### 2.1. *HH 92*

The Very Large Array (VLA) observations were made at 8.46 GHz (3.6 cm) in the B (during epoch 2002 August 1) and A (during epoch 2003 June 21) configurations. The VLA is part of the NRAO<sup>5</sup>. In

<sup>5</sup>The National Radio Astronomy Observatory is operated by Associated Universities Inc. under cooperative agreement with the National Science Foundation.

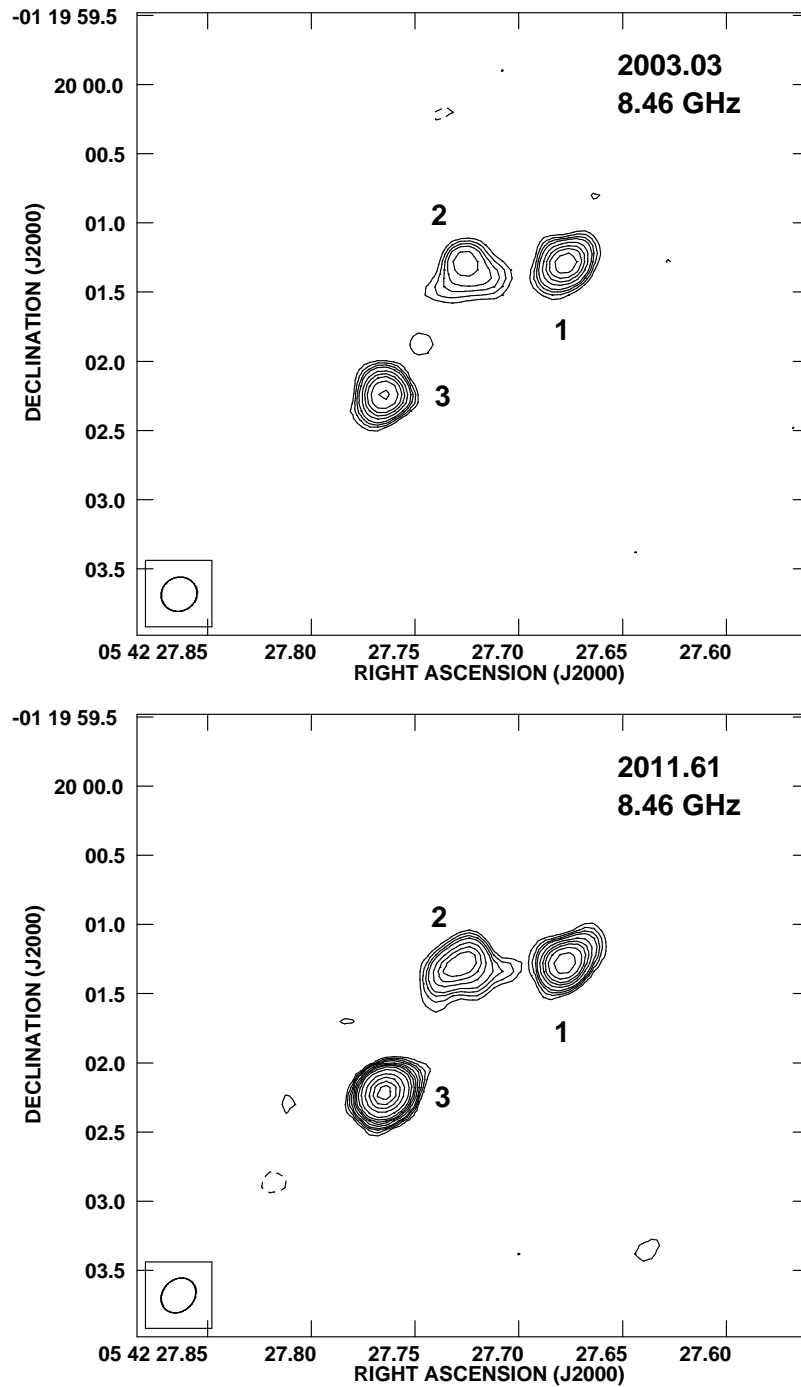


Fig. 2. Contour images of the 8.46 GHz (3.6 cm) continuum emission from the core of the HH 92 outflow. (Top) Image for the 2003.03 epoch. The contours are -4, -3, 3, 4, 5, 6, 8, 10, 12, 15, and 20 times  $12.4 \mu\text{Jy beam}^{-1}$ , the rms noise of the image. The half power contour of the synthesized beam ( $0''.26 \times 0''.24$  with a position angle of  $-62^\circ$ ) is shown in the bottom left corner. (Bottom) Image for the 2011.61 epoch. The contours are -4, -3, 3, 4, 5, 6, 8, 10, 12, 15, 20, 30, 40, 50, and 60 times  $8.9 \mu\text{Jy beam}^{-1}$ , the rms noise of the image. The half power contour of the synthesized beam ( $0''.27 \times 0''.23$  with a position angle of  $-45^\circ$ ) is shown in the bottom left corner.

both epochs the source J1331+305 was used as an absolute amplitude calibrator (with an adopted flux density of 5.21 Jy) and the source J0541-056 was used as the phase calibrator (with bootstrapped flux densities of  $0.879 \pm 0.003$  and  $0.958 \pm 0.007$  Jy for the first and second epochs, respectively). The data were reduced separately for each epoch using the standard VLA procedures and later concatenated to produce images of high sensitivity and high angular resolution. We refer to these concatenated data as having epoch 2003.03, the average epoch of the two observations.

With the purpose of studying the time evolution and kinematics of these sources, we made Expanded Very Large Array (EVLA) observations of the same region during 2011 August 11 in the A configuration. We refer to these data as having epoch 2011.61, 8.58 years after the first observations. The EVLA observations were made at 8.46 GHz (3.6 cm) using two intermediate frequency (IF) bandwidths of 128 MHz each, separated by 128 MHz, and containing both circular polarizations. Each IF was split in 64 channels of 2 MHz each. For the continuum images we averaged the central 54 channels, rejecting five channels at each end of the bandwidth. The data reduction was made using the software package AIPS of NRAO, following the recommendations for EVLA data given in Appendix E of its Cookbook (that can be found at <http://www.aips.nrao.edu/cook.html>). The source J0137+3309 was used as an absolute amplitude calibrator (with an adopted flux density of 3.15 Jy) and the source J0541-056 was used as the phase calibrator (with a bootstrapped flux density of  $0.699 \pm 0.003$ ).

In Figure 2 we show the images of the HH 92 region at the two epochs studied. The top one is made from the 2003.03 data with the  $(u,v)$  weighting parameter ROBUST (Briggs 1995) of the task IMAGR set to -5. The bottom one is made from the 2011.61 data with the  $(u,v)$  weighting parameter ROBUST of the task IMAGR set to 0. The different weightings were needed to produce images of very similar angular resolution, given that the 2003.03 data contains both A and B configuration observations, while the 2011.61 data contains only A configuration observations. These images clearly show three sources that we label as sources VLA 1, 2, and 3. The three sources are distributed in a region of  $\sim 2''$  in extent (830 AU at a distance of 415 pc). In Table 1 we list the parameters of these three sources, taken from the images at both epochs.

## 2.2. HH 34

To obtain an image of the core of HH 34 at 43.3 GHz (7 mm) we used two data sets from the VLA archive. The first data set was taken on 2004 October 05 in the A configuration under project AR552 and the second data set was taken on 2006 August 29 in the B configuration under project AK634. Both observations were made with an effective bandwidth of 100 MHz. For the first epoch 0713+438 was used as flux calibrator (with an adopted flux density of 0.29 Jy) and 0541-056 as phase calibrator, with a bootstrapped flux density of  $0.61 \pm 0.01$  Jy. For the second epoch 1331+305 was used as flux calibrator (with an adopted flux density of 1.45 Jy) and 0541-056 as phase calibrator, with a bootstrapped flux density of  $1.88 \pm 0.06$  Jy. The data were calibrated following the standard VLA procedures for high frequency observations and the two epochs were concatenated to obtain an image with better sensitivity. In Figure 3 we show the resulting image, made with a ROBUST weight of 5 (Briggs 1995) to emphasize sensitivity. An extended source is clearly detected, with peak position  $RA(2000) = 05^h 35^m 29^s.846 \pm 0^s.001$ ,  $DEC(2000) = -06^\circ 26' 58''.08 \pm 0''.02$ , a total flux density of  $3.5 \pm 0.4$  mJy and deconvolved dimensions of  $0''.39 \pm 0''.05 \times 0''.25 \pm 0''.04$ ;  $PA = 55^\circ \pm 13^\circ$ .

## 3. HH 92: RESULTS AND INTERPRETATION

### 3.1. Proper Motions

The positions of the three sources at the two epochs (see Table 1) are approximately coincident within the positional error ( $1\sigma \simeq 0''.01$ ). Using the distance of 415 pc and the time separation of 8.58 years between observations, we set a  $3\text{-}\sigma$  upper limit of  $\leq 7 \text{ km s}^{-1}$  for the proper motions of the sources. This rules out an interpretation in terms of some of them being classic HH knots, since such objects exhibit proper motions an order of magnitude or more larger. Most probably, the radio sources are tracing young stars or stationary HH knots.

### 3.2. Flux Density Variations as a Function of Time

The sources VLA 1 and VLA 2 do not exhibit flux density variations within the observational noise of  $\sim 0.02\text{-}0.03$  mJy. This sets an upper limit of  $\sim 10\%$  to any possible flux density variations. In contrast, source VLA 3 shows a strong increase of a factor of 2, from 0.34 to 0.64 mJy. Furthermore, the deconvolved size of this source decreased for the second epoch, suggesting that most of the flux density increase took place in a very compact region, perhaps due to gyrosynchrotron activity in VLA 3.

TABLE 1  
RADIO SOURCES AT THE CORE OF THE HH 92 OUTFLOW<sup>a</sup>

VLA	Epoch	Position <sup>b</sup>		Total Flux Density (mJy)	Deconvolved Angular Size <sup>c</sup>
		$\alpha$ (J2000)	$\delta$ (J2000)		
1	2003.03	05 42 27.678	-01 20 01.29	0.31±0.02	0''.23 ± 0''.03 × 0''.08 ± 0''.03; +130° ± 9°
1	2011.61	05 42 27.677	-01 20 01.27	0.29±0.02	0''.20 ± 0''.03 × 0''.08 ± 0''.03; +122° ± 10°
2	2003.03	05 42 27.724	-01 20 01.35	0.28±0.03	0''.36 ± 0''.05 × 0''.26 ± 0''.06; +106° ± 34°
2	2011.61	05 42 27.728	-01 20 01.31	0.28±0.02	0''.37 ± 0''.04 × 0''.34 ± 0''.04; +106° ± 12°
3	2003.03	05 42 27.765	-01 20 02.24	0.34±0.02	0''.17 ± 0''.04 × 0''.10 ± 0''.04; +162° ± 28°
3	2011.61	05 42 27.765	-01 20 02.22	0.64±0.02	0''.06 ± 0''.02 × 0''.04 ± 0''.03; +96° ± 45°

<sup>a</sup>Parameters taken from the images at each epoch.

<sup>b</sup>Units of right ascension are hours, minutes, and seconds and units of declination are degrees, arcminutes, and arcseconds. Positional accuracy is estimated to be 0''.01.

<sup>c</sup>Major axis × minor axis; position angle.

### 3.3. Morphology of the Sources

The deconvolved angular dimensions of the sources VLA 2 and VLA 3 are consistent, within noise, with a spherical geometry. In contrast, VLA 1 is clearly elongated, with its major axis  $\sim 3$  times larger than its minor axis. The average position angle of this source (from the two epochs of observation) is  $126^\circ \pm 7^\circ$ , coincident within modulo  $180^\circ$  with the position angle of the optical jet,  $311^\circ$  (Bally et al. 2002).

### 3.4. Interpretation

The resolution of the HH 92 driving source into three radio continuum sources can be interpreted in terms of the sources being either young stars or representing thermal emission from HH shocks. The radio emission could also have a non-thermal origin, as has been observed in the knots of some jets (e.g. Carrasco-González et al. 2010), but we do not have the multifrequency data required to test this possibility.

Recent submm observations using the SMA interferometer by Chiang et al. (in prep.) have revealed that there is only one  $850 \mu\text{m}$  source in the field of the triple system, namely VLA 1. Neither VLA 2 nor VLA 3 are detected. This strongly suggests that VLA 1 is the driving source, and is consistent with the elongation along the flow axis seen for VLA 1 (see above).

So what are VLA 2 and 3? Both lie approximately within the redshifted outflow lobe from VLA 1, which would indicate that they are HH

knots. However, our two-epoch observations spanning  $8 \frac{1}{2}$  yr reveal no measurable proper motions at all, and put very stringent limits on the proper motions of less than  $7 \text{ km s}^{-1}$ . Since HH flows typically have space velocities of  $100 \text{ km s}^{-1}$  or more, such slow motions would indicate that the motion is mostly along the line of sight. However, this is inconsistent with the giant flow dimensions of about 3 pc, which points towards an outflow axis lying close to the plane of the sky. It follows that if VLA 2 and 3 are shocks, then they are stationary shocks, such as would occur if small ambient cloudlets are interacting with a strong stellar wind or outflow (Schwartz 1978). Possible stationary shocks with no detectable proper motions along the flow have been found in regions of high ambient density (e.g., Martí et al. 1995; Rodríguez et al. 2008b). This interpretation gains weight because at least VLA 3 shows strong flux-variability over the time span of the observations.

Alternatively, a possible scenario would be that the HH 92 driving source forms a small non-hierarchical triple stellar system, and that an outflow from the active source VLA 1 runs over the two nearby stellar components of the triple system, creating shocks where the outflow rams into the circumstellar material of these two stars. A similar case has recently been identified in the young IRAS 162932422 triple system (Girart et al. 2014). This scenario is not inconsistent with the lack of detection of VLA 2 and 3 at submm wavelengths, because not all very young stars are detectable at sub-mm wavelengths, since the cool circumstellar envelopes merely

re-emit instantaneously the radiation from the central protostars, and if the accretion is dormant, the re-emission from the envelopes will be weak.

The presently available observations do not allow us to distinguish between the two scenarios in which VLA 2 and 3 are either small cloudlets or protostellar companions.

#### 4. HH 34: RESULTS AND INTERPRETATION

Our 7 mm map of the HH 34 driving source is seen in Figure 3. When compared to the beam, the source is clearly extended in a NE-SW direction, but there is also an extension almost perpendicular to the main elongation. In Figure 4 we show the area of our 7 mm map shown in Figure 3 as a square superposed on a high-resolution optical image ([SII] 6717/6731 transitions) of the HH 34 jet. It is immediately evident that the main elongation of the source is perpendicular to the jet axis, suggesting that what we see is dust emission from a circumstellar disk. The disk has a total width of 0.4 arcsec, which corresponds to a radius of  $\sim 80$  AU, matching well with expectations for Class I disks. At 7 mm, both dust emission and free-free emission can be detected (Rodríguez et al. 2008a), and so it seems likely that the elongation we see perpendicular to the disk axis results from the jet, which is monopolar at optical wavelengths, but bipolar at mid-infrared wavelengths (Raga et al. 2011).

We estimate the total mass of the 7 mm source by assuming optically thin, isothermal dust emission and a gas-to-dust ratio of 100 (Sodroski et al. 1997). The total mass opacity coefficient at 7 mm is poorly known and values between  $8 \times 10^{-3} \text{ cm}^2 \text{ g}^{-1}$  (Rodríguez et al. 2007) and  $2 \times 10^{-3} \text{ cm}^2 \text{ g}^{-1}$  (Isella et al. 2014) can be found in the literature. Assuming an average value of  $5 \times 10^{-3} \text{ cm}^2 \text{ g}^{-1}$ , the total mass can be roughly estimated to be:

$$\left[ \frac{M}{M_{\odot}} \right] = 0.17 \left[ \frac{S_{\nu}}{mJy} \right] \left[ \frac{T}{100 \text{ K}} \right]^{-1} \left[ \frac{D}{kpc} \right]^2,$$

where  $S_{\nu}$  is the flux density at 7 mm,  $T$  is the dust temperature and  $D$  is the distance to the source. Assuming  $T = 50$  K and a distance of 416 pc, we estimate a mass of  $\sim 0.21 M_{\odot}$  for the HH 34 disk.

Almost precisely  $\sim 0''.4$  north of the HH 34 source there is a weak signal, which is possibly real since it is detected at a  $4\text{-}\sigma$  level, but which will require confirmation from additional observations. If real, it is located 180 AU in projection from the main source. Reipurth (2000) has suggested that all giant HH flows are the result of dynamical interactions

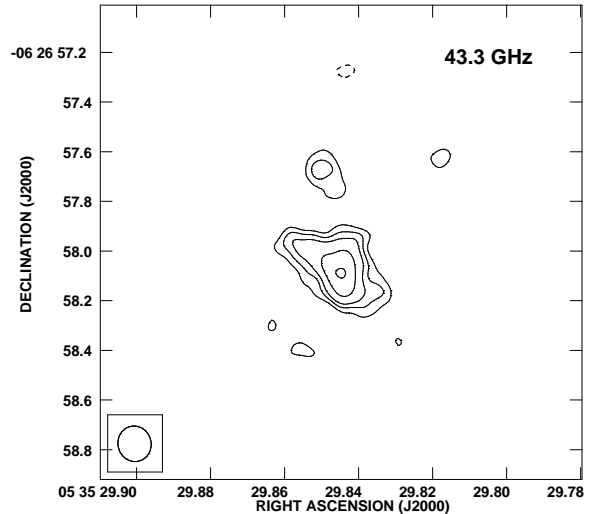


Fig. 3. A 43.3 GHz (7 mm) radio continuum map of a  $1.9'' \times 1.9''$  area around the HH 34 driving source. The elongation of the source is perpendicular to the jet axis as seen in Figure 4 and is likely to represent cool dust in a circumstellar disk. At the assumed distance of 416 pc, the  $0.4''$  width of the disk corresponds to about 160 AU. The contours are  $-4, -3, 3, 4, 5, 7,$  and  $9$  times  $77 \mu\text{Jy beam}^{-1}$ , the rms noise of the image. The half power contour of the synthesized beam ( $0''.14 \times 0''.13$  with a position angle of  $14^\circ$ ) is shown in the bottom left corner.

in and disintegration of triple or small multiple systems. In this interpretation, the HH 34 source should be a close binary with separation of order 10 AU. No existing data of the HH 34 source has sufficient spatial resolution to detect such a close binary. In addition to the companion possibly detected here, another very faint companion (“HH 34 X”) was detected in the K-band with HST by Reipurth et al. (2000), about  $5''$  west of the jet source. Finally, a faint variable star (“Star B”) is located  $11''$  SE of the driving source and seen at the left edge of Fig. 4 (Reipurth et al. 1986, 2002b). Altogether, the HH 34 driving source may have several more distant companions.

#### 5. CONCLUSIONS

We have presented VLA and EVLA observations made at 8.46 GHz (3.6 cm) of the core of the HH 92 outflow, made at two epochs separated by 8.58 years. We detect a group of three compact radio sources, of which VLA 1 drives the HH 92 jet. The other two sources, VLA 2 and 3, may be stationary shocks surrounding either small cloudlets or protostars.

Additional VLA observations obtained at 7 mm of the driving source of the HH 34 jet have revealed

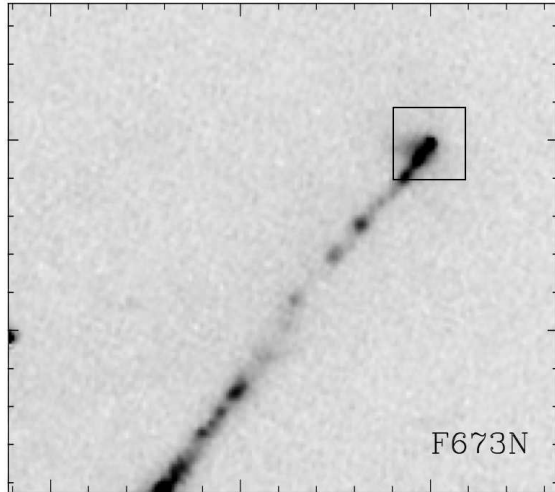


Fig. 4. A WFPC2 HST image of the base of the HH 34 jet obtained through a narrow-band filter transmitting the [SII] 6717/6731 doublet lines. Tick marks are in steps of one arcsec, and the field of view is about  $12'' \times 14''$ . The box outlines the  $1.9'' \times 1.9''$  field shown in 7 mm radio continuum in Figure 3. Image from Reipurth et al. (2002b).

a circumstellar disk perpendicular to the jet axis and with a radius of  $\sim 80$  AU and mass of  $\sim 0.21 M_{\odot}$ .

LFR acknowledges the support of DGAPA, UNAM, and of CONACyT (México). BR and HFC acknowledge support by the National Aeronautics and Space Administration through the NASA Astrobiology Institute under Cooperative Agreement No. NNA09DA77A issued through the Office of Space Science. This research has made use of the SIMBAD database, operated at CDS, Strasbourg, France.

#### REFERENCES

- Anglada, G. 1996, in ASP Conf. Ser. 93, Radio Emission from the Stars and the Sun, ed. A. R. Taylor & J. M. Paredes (San Francisco: ASP), 3
- Anthony-Twarog, B. J. 1982, AJ, 87, 1213
- Bally, J., Reipurth, B., & Aspin, C. 2002, ApJ, 574, L79
- Briggs, D. 1995, Ph.D. thesis, New Mexico Inst. of Mining and Technology
- Chiang, H.-C., Reipurth, B., & Lee, C.-F., in prep.
- Carrasco-González, C., Rodríguez, L. F., Anglada, G., et al. 2010, Science, 330, 1209
- Curiel, S., Rodríguez, L.F., Moran, J.M., Cantó, J. 1993, ApJ, 415, 191
- Davis, C. J., Mundt, R., & Eisloffel, J. 1994, ApJ, 437, L55
- Devine, D., Bally, J., Reipurth, B., & Heathcote, S. 1997, AJ, 114, 2095
- Di Francesco, J., Johnstone, D., Kirk, H., MacKenzie, T., & Ledwosinska, E. 2008, ApJS, 175, 277
- Duchêne, G., Delgado-Donate, E., Haisch Jr, K. E., Loinard, L. & Rodríguez, L. F. 2006, in Protostars and Planets V, ed. B. Reipurth, D. Jewitt, & K. Keil (Tucson: Univ. Arizona Press), 379.
- Dzib, S. A., Loinard, L., Mioduszewski, A. J., et al. 2013, ApJ, 775, 63
- Girart, J.M., Estalella, R., Palau, A., Torrelles, J.M., & Rao, R. 2014, ApJ, 780, L11
- Gredel, R., Reipurth, B., & Heathcote, S. 1992, A&A, 266, 439
- Herbig, G.H. 1974, Lick Obs. Bull. No. 658
- Isella, A., Chandler, C. J., Carpenter, J. M., Pérez, L. M., & Ricci, L. 2014, arXiv:1404.5627
- Kim, M.K., Hirota, T., Honma, M. et al. 2008, PASJ, 60, 991
- Lada, E.A., Bally, J., Stark, A.A. 1991, ApJ, 368, 432
- Manoj, P., Watson, D.M., Neufeld, D.A. et al. 2013, ApJ, 763:83
- Martí, J. Rodríguez, L. F., & Reipurth, B. 1995, ApJ, 449, 184
- Megeath, S.T., Gutermuth, R., Muzerolle, J. et al. 2012, AJ, 144:192
- Menten, K.M., Reid, M.J., Forbrich, J. & Brunthaler, A. 2007, A&A, 474, 515
- Miettinen, O. & Offner, S.S.R. 2013, A&A, 553:A88
- Muench, A., Getman, K., Hillenbrand, L. & Preibisch, T. 2008, in *Handbook of Star Forming Regions, Vol. I*, ed. Bo Reipurth (San Francisco: ASP Monograph Publications), 483
- Raga, A.C., Noriega-Crespo, A., Lora, V., Stapelfeldt, K.R., & Carey, S.J. 2011, ApJ, 730, L17
- Reipurth, B. 1985, A&AS, 61, 319
- Reipurth, B. 1989, A&A, 220, 249
- Reipurth, B. 2000, AJ, 120, 3177
- Reipurth, B., Bally, J., Graham, J.A., Lane, A.P., & Zealey, W.J. 1986, A&A, 164, 51
- Reipurth, B., Yu, K.C., Heathcote, S., Bally, J., & Rodríguez, L.F. 2000, AJ, 120, 1449
- Reipurth, B., Chini, R., Krügel, E., Kreysa, E., & Sievers, A. 1993, A&A, 273, 221
- Reipurth, B., Rodríguez, L. F., Anglada, G., & Bally, J. 2002a, AJ, 124, 1045
- Reipurth, B., Heathcote, S., Morse, J., Hartigan, P., & Bally, J. 2002b, AJ, 123, 362
- Reipurth, B., Rodríguez, L. F., Anglada, G., & Bally, J. 2004, AJ, 127, 1736
- Reipurth, B., Clarke, C.J., Boss, A.P., Goodwin, S.P., Rodríguez, L.F., Stassun, K.G., Tokovinin, A., & Zinnecker, H. 2014, in *Protostars and Planets VI*, eds. H. Beuther, R. Klessen, C. Dullemond, Th. Henning, in press (arXiv: 1403.1907)
- Rodríguez, L. F. 1997, in Herbig-Haro Flows and the Birth of Low Mass Stars, proceedings of IAU Symp. No. 182, eds. B. Reipurth & C. Bertout, p. 83 (Dordrecht: Kluwer)
- Rodríguez, L.F. & Reipurth, B. 1996, Rev. Mex. Astron. Astrofis., 32, 27
- Rodríguez, L. F., Delgado-Arellano, V. G., Gómez, Y.,

- Reipurth, B., Torrelles, J. M., Noriega-Crespo, A., Raga, A. C., & Cantó, J. 1999, *AJ*, 119, 882
- Rodríguez, L. F., Zapata, L. A., & Ho, P. T. P. 2007, *ApJ*, 654, L143
- Rodríguez, L. F., Torrelles, J. M., Anglada, G., & Reipurth, B. 2008a, *AJ*, 136, 1852
- Rodríguez, L. F., Moran, J. M., Franco-Hernández, R., et al. 2008b, *AJ*, 135, 2370
- Schwartz, R.D. 1978, *ApJ*, 223, 884
- Sodroski, T. J., Odegard, N., Arendt, R. G., et al. 1997, *ApJ*, 480, 173

Luis F. Rodríguez: Centro de Radioastronomía y Astrofísica, UNAM, A. P. 3-72, (Xangari), 58089 Morelia, Michoacán, México (l.rodriguez@crya.unam.mx).

Bo Reipurth: Institute for Astronomy, University of Hawaii at Manoa, 640 North Aohoku Place, Hilo, HI 96720, USA (reipurth@ifa.hawaii.edu).

Hsin-Fang Chiang: Institute for Astronomy, University of Hawaii at Manoa, 640 North Aohoku Place, Hilo, HI 96720, USA (hchiang@ifa.hawaii.edu).